Available online at www.sciencedirect.com
ScienceDirect
Journal of Sound and Vibration 311 (2008) 200–211
JOURNAL OF SOUND AND VIBRATION
www.elsevier.com/locate/jsvi

Design and analysis of auto-balancer of an optical disk drive using speed-dependent vibration absorbers

C.C. Cheng*, F.T. Wu, K.S. Hsu, K.L. Ho

Department of Mechanical Engineering, National Chung Cheng University, Chia-Yi 621, Taiwan, ROC

Received 9 January 2007; received in revised form 1 August 2007; accepted 30 August 2007
Available online 17 October 2007

Abstract

With the increased demands in performance, the optical disk drive needs to be high speed and more stable. A novel design of a vibration absorber used in reducing the vibration caused by the imbalance of an optical disk drive is proposed. When an optical disk is rotating, the vibration caused by the imbalance resulting from the non-homogeneous disk increases as the rotating speed increases. The proposed vibration absorber with a circular shape is installed beneath the optical disk. It rotates with the disk; therefore its natural frequency varies with the rotating speed due to the change of in-plane stress caused by the centrifugal force. The objective is to use shape optimization technique to make the first radial natural frequency of the absorber coincide with the rotating speed of the optical disk in a specific frequency range. Under this circumstance, the natural frequency of the absorber becomes speed-dependent and the absorber will keep resonant in this specific frequency range. It can effectively suppress the vibration in the radial direction caused by the imbalance of the optical disk and acts as an auto-balancer. Results from experiments and numerical simulations using finite element method both show that the imbalance of the optical disk can be reduced effectively.

1. Introduction

Increasing the data storage capacity of an optical disk accompanied by the demands of high data access rates and high positioning accuracy of read/write heads has recently become a stringent necessity. With the increased demands in performance, the optical disk drive (ODD) needs rotating with high speed and more stability.

The optical disk possesses a certain degree of imbalance due to material inhomogeneity or manufacturing tolerance. This imbalance causes severe radial vibration when the disk is rotating at a high speed. In order to suppress the excessive radial vibrations caused by the imbalance, the automatic ball-type balancer system (ABB) which consists of several free-moving ball-type masses running in specific circular races around the rotor is utilized. The ball-type masses in ABB tend to settle at positions to counter-balance the disk imbalance when the motor spindle is rotating. Owing to its simple mechanism, the ABB becomes a favorable device for reducing the imbalance in an optical disk drive system. Several implementations and novel designs were

*Corresponding author. Tel.: +886 5 2720411x33313; fax: +886 5 2720589.
E-mail address: imeccc@ccu.edu.tw (C.C. Cheng).

0022-460X/$ - see front matter
doi:10.1016/j.jsv.2007.08.038

proposed and patented [1–3]. Several studies have been conducted, either experimentally or theoretically, in order to have a better understanding of the dynamic characteristics of the ABB [4–6]. Some issues, such as rolling friction of balancing balls [5,6], effectiveness limitation caused by rotating speed [7], instability [4], etc. still need to be addressed when an optical disk drive system is equipped with an ABB. For example, the ball mis-positioning caused by the rolling friction hampers the effectiveness of the ABB and sometimes even results in an excess vibration.

A novel design of a dynamic balancer is proposed in this paper to reduce the vibration caused by the imbalance of an optical disk drive and it provides an alternative besides the ABB. The proposed dynamic balancer is in fact a circular structure and is installed beneath the optical disk. It rotates with the optical disk; therefore its natural frequency varies with the rotating speed due to the change of in-plane stress caused by the centrifugal force. The idea is to make the varying first radial natural frequency of this rotating circular structure coincide with the rotating speed of the optical disk in a specific rotational speed range. Under this circumstance, the dynamic balancer will keep resonant and act as a vibration absorber in this specific frequency range. Theoretically it can effectively suppress the vibration in the radial direction of the rotor-disk system caused by the imbalance. Although the mechanism of a vibration absorber in reducing the vibration caused by the imbalance is different from that of ABB, it serves the same purpose of reducing the imbalance of the rotor-disk system. As compared to the ABB, it does not have the shortcoming of mis-position caused by the rolling friction and instability. And most of all, it has a much simpler mechanism and can be fabricated using a mold machine in a cost-effective manufacturing process.

2. Design concept of speed-dependent vibration absorber

The vibration absorber has been proved to be effective in reducing the machine vibration [8,9]. Fig. 1 shows a typical dynamic response of a machine before and after the vibration absorber is implemented, in which ω_n is the natural frequency of the machine, ω_a is the natural frequency of the absorber, and ω is the excitation frequency. By simply attaching a vibration absorber to a machine and tuning its natural frequency to that of the machine, the original resonance of the machine disappears. However, two new natural frequencies where resonances may occur take place instead. When the new resonances occur, the absorber vibrates in phase and out of phase with respect to the machine, respectively. If the machine operates at a frequency between these two new natural frequencies, the machine vibration can be reduced dramatically. When the natural frequency of the absorber is not exactly identical to that of the machine, one of the new resonances will shift toward the

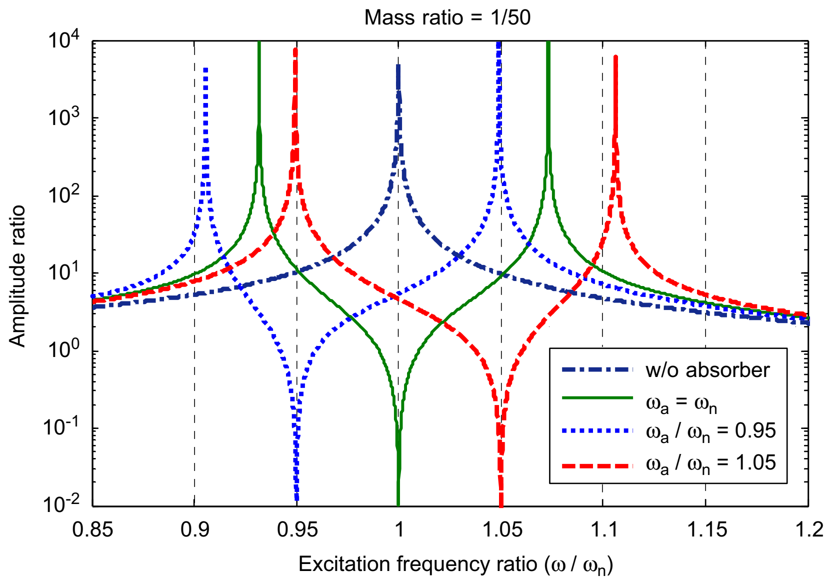

Fig. 1. The dynamic response of the machine with/without the vibration absorber.

excitation frequency as shown by the dash line and the dot line in Fig. 1. It is well known that the frequency range between the two natural frequencies depends on the mass of the vibration absorber as compared to that of the machine itself. Usually the machine operates at the natural frequency of the absorber and enjoys a great vibration reduction. A wide frequency range between the two natural frequencies is preferred in order to avoid situations where excitation frequency might drift around the nominal value. One may use a heavier absorber to increase the operating frequency range; however, the weight of vibration absorber is always limited in the design.

If the natural frequency of a vibration absorber can be tuned in such a way that it changes in accordance with the varying excitation frequency, the vibration absorber may become more effective in a wide frequency range. It is also well-known that the excitation frequency for a typical rotary machine caused by imbalance is the same as the rotating speed of its own shaft. If the natural frequency of a vibration absorber is designed to be the same as the rotating speed of the shaft and can also adapt itself to follow the varying rotating speed, under this circumstance, the vibration absorber will have its best performance in countering the imbalance in a wide frequency range. The question is how to design a vibration absorber that changes its own natural frequency in accordance to the varying rotating speed?

It is well-known that the natural frequency of a rotating structure will change due to the centrifugal force [10,11]. The stress stiffening effect caused by the centrifugal force increases the structural bending rigidity and thus it tends to increase the natural frequency of the rotating structure. On the contrary, the same centrifugal force increases the structure length and thus it tends to decrease the natural frequency of the rotating structure, i.e. the spin softening effect. Compared with the stress stiffening effect, the spin softening influences the disk response only in the plane of rotation. Inspired by the phenomenon of the varying natural frequency of a structure due to the rotational effect, a speed-dependent vibration absorber, called SDVA hereafter, is proposed to suppress the imbalance caused by the optical disk at varying rotating speed.

In order to fulfill the requirement of self-tuning the natural frequency at a varying disk rotating speed, a SDVA as shown in Fig. 2 is introduced. It has a simple, circular geometry and is designed to be installed beneath the disk, which is also the same place for the traditional ABB. This SDVA consists of several ribs connected by a rim. When the SDVA is rotating with the shaft, each rib behaves like a rotating beam of which bending stiffness will increase due to the centrifugal force and thus its natural frequency can be altered. On the contrary, the rim acts as a tip mass and is designed not only to create an inertia effect but also to restrain the tip deflection of the rib, so it may not interfere with the disk in rotation. Its appearance makes the natural frequency of the absorber more tunable. Note that the vibration absorber possesses different kinds of modes that depend on the excitation frequency. Among all the vibration mode, the radial mode that represents the vibration absorber vibrates in the radial direction is the only vibration motion to be utilized to counter the disk imbalance. Therefore the objective is to make the radial natural frequency of SDVA vary in accordance with the disk rotating speed. To accomplish this task, an optimal algorithm based on the shape optimization technique is developed to find the dimension of SDVA to ensure that the natural frequency corresponding to the first radial mode of SDVA matches with the rotating speed in a specific frequency range, i.e. 6000–10,200 rev/min for SDVA in this study.

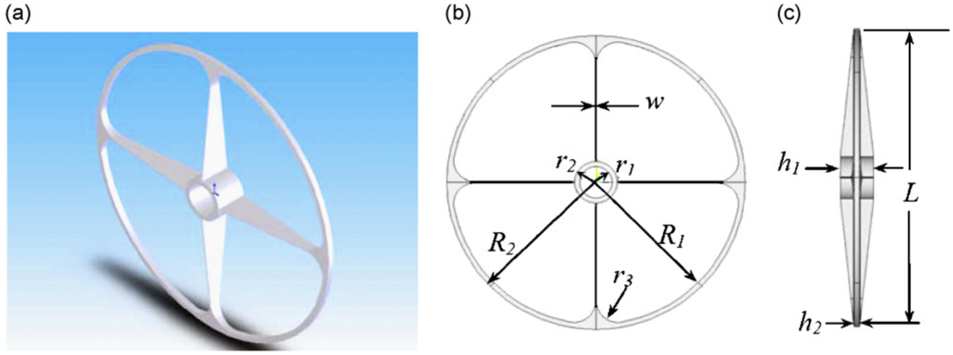

Fig. 2. The proposed speed-dependent vibration absorber (SDVA); (a) 3-D view, (b) front view and (c) side view.

3. Shape optimization of speed-dependent vibration absorber

Shape optimization involves the determination of parts of or all of the profiles of the absorber boundaries. Generally there are two ways to describe the profile of a structure. One is to represent the structural shape by a set of mathematical functions, e.g. geometric modeling using B-Spline curves; the other is to describe the profile using discrete points. The design variables are the coefficients corresponding to the mathematical functions in the first approach; and the position corresponding to each of the discrete point in the second. In this study, the design variables of the absorber as illustrated in Fig. 2 are: h_1 the inner rim thickness, h_2 the outer rim thickness, r_1 the inside radius of inner rim, r_2 the outside radius of inner rim, R_1 the inside radius of outer rim, R_2 the outside radius of outer rim and w the rib width. With these design variables the shape optimization problem can be simplified to be a size optimization defined as follows:

Minimize

$$F_2(x_1, x_2, \dots, x_j, \dots, x_n) = \sum_{i=1}^{m} (\omega_i - \Omega_i)^2 \quad \text{for} \quad \Omega_l \leqslant \Omega_i \leqslant \Omega_u, \tag{1a}$$

subject to

$$L_{lj} \leqslant x_j \leqslant L_{uj}, \tag{1b}$$

where x_j is the design variable, n is the total number of the design variables, Ω_i is the shaft rotating speed in Hz, ω_i is the natural frequency in Hz corresponding to the first radial mode of the vibration absorber at the rotational speed Ω_i, m is the total number of the discretized rotating speed from $\Omega_l = 100$ Hz (6000 rev/min) to $\Omega_u = 170$ Hz (10,200 rev/min) for SDVA, L_{lj} and L_{uj} represent the lower and upper bounds for each design variable x_j due to space limitation in an ODD. To accomplish the design task, the commercial finite element package ANSYS is used due to the complexity of structure.

As a first step, a numerical algorithm, which incorporates finite element code ANSYS, mathematical subroutines IMSL libraries and the user-supplied routines is developed. The advantage is simply that it extends the capability and flexibility of ANSYS. ANSYS calculates the responses of a complicate structure such as stress distribution, dynamic response, etc., whereas IMSL is responsible for providing subroutines including optimization, transformations, matrix operations, etc. The user-supplied subroutine is required for calculating the objective function, interfacing between IMSL and ANSYS; and controlling the iteration. In other words, this algorithm provides a general and an automatic procedure in a general optimization framework. Among all the optimization methods, the sub-problem approximation technique was chosen to perform the optimization procedure. It has the advantage that the derivatives of the objective function are not required, i.e. a zero-order method. One may choose other zero order method, such as the principal axis method to accomplish the same task [12,13].

4. Numerical results and discussions

Assume that the SDVA is made of polyurethane (PU) with a Young's modulus $E = 0.012 \times 10^9$ Pa, Poisson's ratio $v = 0.45$ and density $\rho = 960\,\text{kg/m}^3$. The dimension of the SDVA before size optimization is listed in Table 1. The first four mode shapes are illustrated in Fig. 3. The first mode is easily identified as the torsional mode with four ribs bending in phase circumferentially. The second mode is a radial mode where two opposite ribs bend in phase; and the other two opposite ribs vibrate longitudinally. In this mode the rim of the SDVA vibrates in the radial direction and is similar to the motion of a disk caused by the imbalance. The third mode is also a radial mode whose natural frequency is a little higher than the second mode; however, in this

Table 1
Dimensions of SDVA before optimization (unit: mm)

R_1	R_2	r_1	r_2	w	h_1	h_2	r_3	L
13.5	14	1.5	2	0.1	3	0.3	2	28

mode two adjacent ribs bend out of phase. The rim of SDVA moves in the direction of 45° relative to rib axial direction. The fourth mode is a flexural mode although it can hardly be seen from the top view as shown in Fig. 3(d). It is obvious that the second mode which exhibits vibration in the radial direction is the best choice to be used to counter the imbalance caused by the rotating disk. Therefore the objective in designing a SDVA is to vary its natural frequency corresponding to this radial mode in accordance with the disk rotational speed in a specific rotational speed range. Under this circumstance, ideally the vibration absorber will keep resonant at different disk rotating speeds and theoretically acts as an auto-balancer to counteract the imbalance caused by the disk.

By utilizing the algorithm which incorporates the ANSYS and the IMSL introduced in the previous section, the SDVA was optimized subject to inequality constraints due to space limitation as listed in Table 2.

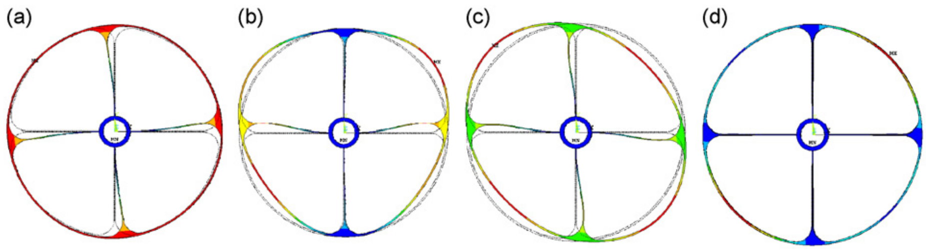

Fig. 3. The first four mode shapes of vibration absorber at 6000 rev/min before optimization; (a) the 1st mode, (b) the 2nd mode, (c) the 3rd mode and (d) the 4th mode.

Table 2
Constraints of SDVA used in optimization (unit: mm)

	R_1	R_2	r_2	r_3	w	h_1	h_2
Low bound	13	13.1	1.7	0.5	0.1	0.3	0.3
Upper bound	15.4	15.5	6	3.5	0.4	3.8	3.8

Table 3
Dimensions of SDVA after optimization (unit: mm)

	R_1	R_2	r_1	r_2	r_3	w	h_1	h_2
SDVA I	15.18	15.28	1.5	4.9	1.6	0.14	3.8	0.52
SDVA II	15.8	16.8	1.5	4.0	2.0	1.0	3.8	1.0
SDVA III	15.9	16.9	1.5	2.5	2.8	1.0	3.9	1.0

Table 4
Natural frequencies and mode shapes of SDVA I at varying rotational speeds

	Mode 1 (Torsional)	Mode 2 (1st Radial)	Mode3 (2nd Radial)
0 rev/min (0 Hz)	15.396 Hz	23.797 Hz	25.633 Hz
6000 rev/min (100 Hz)	66.397 Hz	106.62 Hz	111.47 Hz
7020 rev/min (117 Hz)	76.265 Hz	121.65 Hz	127.50 Hz
8040 rev/min (134 Hz)	86.144 Hz	136.48 Hz	143.45 Hz
9000 rev/min (150 Hz)	95.444 Hz	150.24 Hz	158.38 Hz
10,200 rev/min (170 Hz)	105.32 Hz	164.64 Hz	174.14 Hz

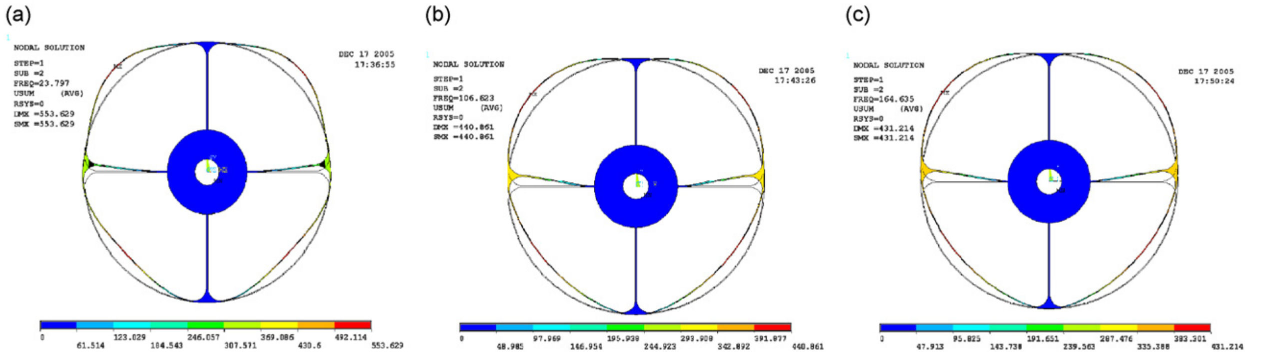

Fig. 4. The first radial mode of SDVA I at different rotational speeds after optimization; (a) 0 rev/min, (b) 6000 rev/min and (c) 10,200 rev/min.

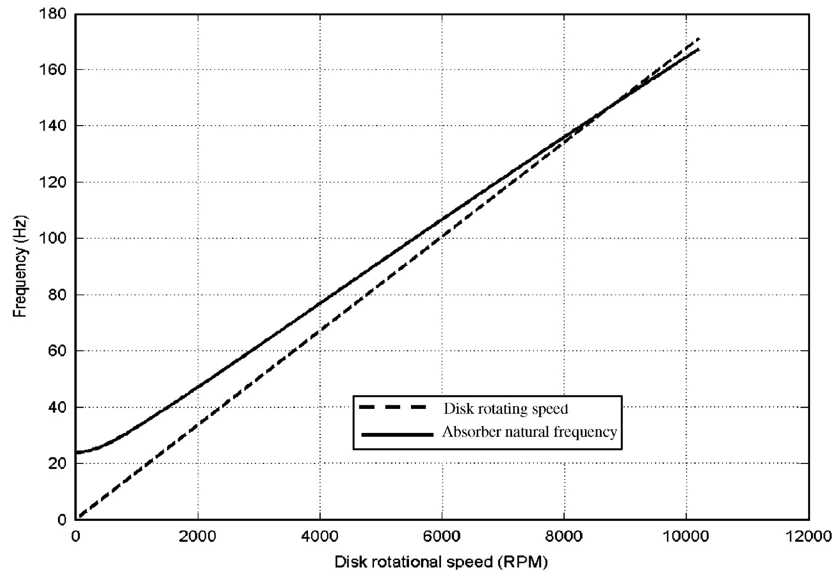

Fig. 5. The natural frequency corresponding to the 2nd mode of the SDVA I at varying rotating speeds.

The final dimension of SDVA, denoted by SVDA I hereafter, after optimization is listed in Table 3. The natural frequency corresponding to the second mode of the SDVA I after size optimization at rotating speeds of 0, 6000, 7020, 8040, 9000 and 10,200 rev/min is listed in Table 4; and the corresponding mode shape are shown in Fig. 4. It shows that the SDVA I exhibits the same mode shape where two opposite ribs exhibit in-phase bending and the other two opposite ribs vibrate longitudinally during the disk run-up from 6000 to 10,200 rev/min. The natural frequency corresponding to this radial mode during the disk run-up is shown in Fig. 5. In this figure, note that the natural frequency of the second mode of the SDVA I varies in accordance with the disk rotational speed in the range from 6000 to 10,200 rev/min with a discrepancy less than 6.6 Hz. This result numerically validates that the radial natural frequency of the SDVA I can be altered to approximately match with the disk rotating speed. Now the question left is how the SDVA performs if it is installed in an optical disk drive.

5. Performances study of SDVA acting as auto-balancer

To evaluate the performance in vibration reduction of the proposed SDVA I used as auto-balancer on an optical disk drive, a numerical example is presented.

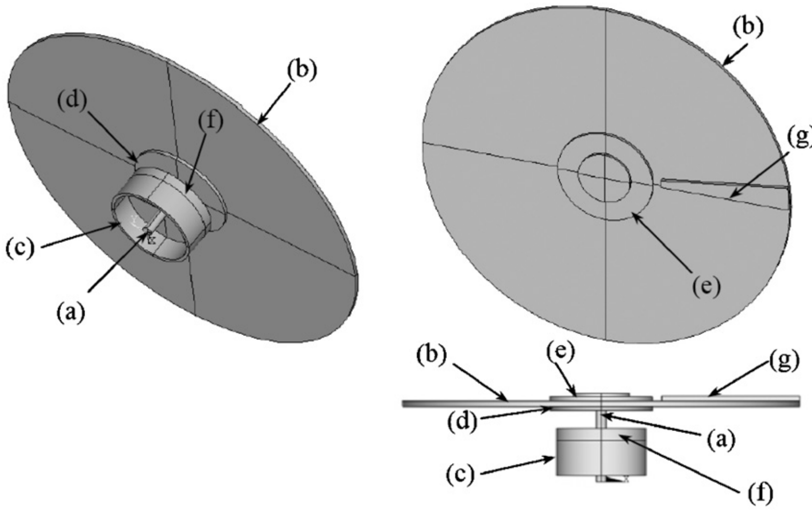

Fig. 6. Rotor-disk model; (a) spindle, (b) disk, (c) sleeve, (d) turntable, (e) clamp, (f) washer and (g) imbalance.

Table 5
Material properties of a simplified disk drive

Components	Material	Young's modulus (Pa)	Density (kg/m^3)
Disk	Plastic	2.16×10^9	1200
Spindle	Steel	1.9×10^{11}	7850
Sleeve	Aluminium	7.2×10^{10}	2800
Washer	Rubber	4×10^6	1300
Turntable	Aluminium	7.2×10^{10}	2800
Clamp	Plastic	1.4×10^9	960
Imbalance	Plastic	2.16×10^9	1200

As shown in Fig. 6, a finite element model according to an optical disk drive is created using the commercial package ANSYS. Owing to the complexity of a real optical disk drive, this finite element model is simplified and consists of only the key components which are a spindle, a disk, a turntable, a sleeve, a washer and a clamp. In addition, the disk is assumed to have an imbalance of 3 g. The material property for each component is listed in Table 5. The optical disk is fixed at its inner circle by a clamp on the turntable but the disk is free to rotate with the turntable and the clamp without slip due to the washer. Similarly, the displacement at the bottom of the spindle is assumed to be fixed both in the axial and radial directions but it is free to rotate in the axial direction. This finite element model was meshed using 22,856 elements of solid 45 in ANSYS.

Fig. 7 shows the natural frequency of the rotor-disk system at varying rotational speed. It shows that the natural frequencies corresponding to the bending modes increase with respective to the increasing disk rotational speed; however, the natural frequency of torsional mode almost remains the same. The frequency response of the disk caused by the imbalance can be determined straightforward. The non-dimensional radial displacement responses, $(MX)/(me)$ at the outer rim of the disk with and without the SDVA I are shown in Fig. 8 for the rotating speed from 0 to 10,200 rev/min, where $M = 19$ g is the total mass of the disk with the imbalance included, $m = 3$ g is the imbalance mass, $e = 4.3$ cm is the distance from the imbalance to mass center and X is the disk radial displacement at outer rim of the disk. It shows that the radial vibration is obviously reduced with the SDVA I being installed as expected, especially at the frequency ranging from 4000 to 7000 rev/min where three vibration peaks are suppressed. These vibration peaks, as shown in Fig. 8, two are located in the frequency range from 4000 to 6000 rev/min and one is at approximately 6900 rev/min can be

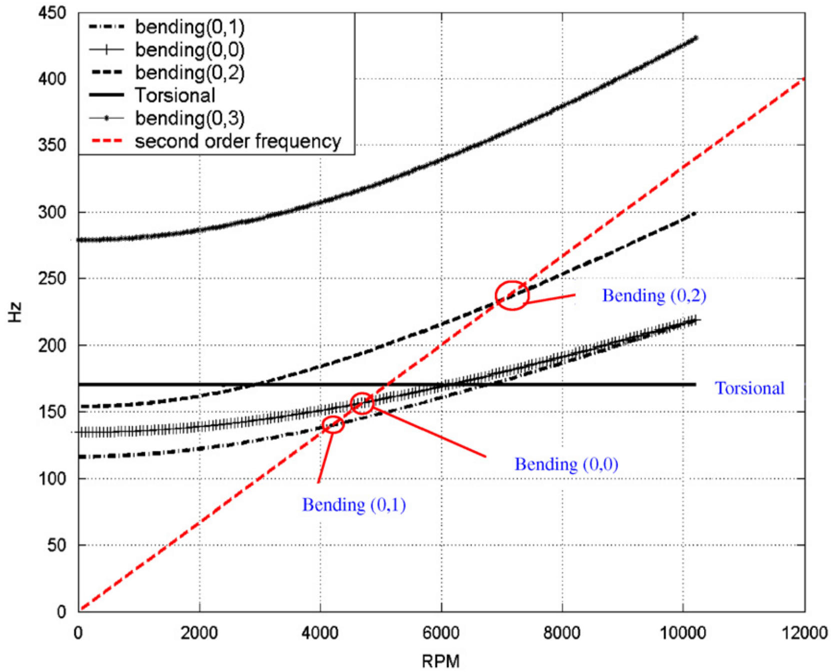

Fig. 7. The natural frequency of rotor-disk model at varying rotating speeds.

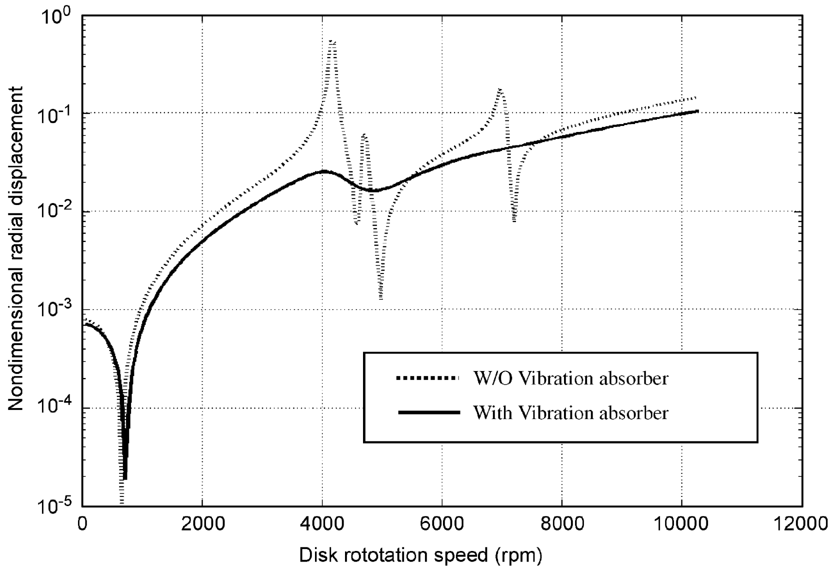

Fig. 8. Comparisons of disk radial vibration displacement before and after SDVA I being installed.

identified from Fig. 7 as the resonances corresponding to first three bending modes of rotor-disk system. Although the SDVA I was optimized according to the disk rotational speed in the range from 6000 to 10,200 rev/min, the discrepancy in the frequency between the rotating speed and the natural frequency of the first radial mode of SDVA I is approximately only 10 Hz at 4000 rev/min as shown in Fig. 5. With the small natural frequency ratio $\omega_a/\omega_n = 1.15$ of the vibration absorber to the rotor-disk system, the SDVA I still effectively suppresses the imbalance in the range from 4000 to 6000 rev/min where two bending resonances occur.

From the result of numerical simulation, the SDVA I can effectively suppress the vibration due to imbalance in a wide range of the rotating speed; however, difficulty encountered in fabrication due to its small dimensions of the rib and the rim. Two new types of SDVA, denoted by SDVA II and SDVA III hereafter, were obtained after size optimization and will be tested experimentally to validate their performances in reducing the vibration due to disk imbalance. Table 3 lists the dimensions of SDVA II and SDVA III, and Table 6 lists their material properties. The SDVA II was optimized for the lower rotational speed ranged from

Table 6
Material properties of SDVA

	Young's modulus (Pa)	Density (kg/m^3)	Poisson's ratio	Mass (g)
SDVA I	0.012×10^9	960	0.45	0.25
SDVA II	0.002×10^9	1220	0.45	0.5
SDVA III	0.035×10^9	1220	0.45	0.4

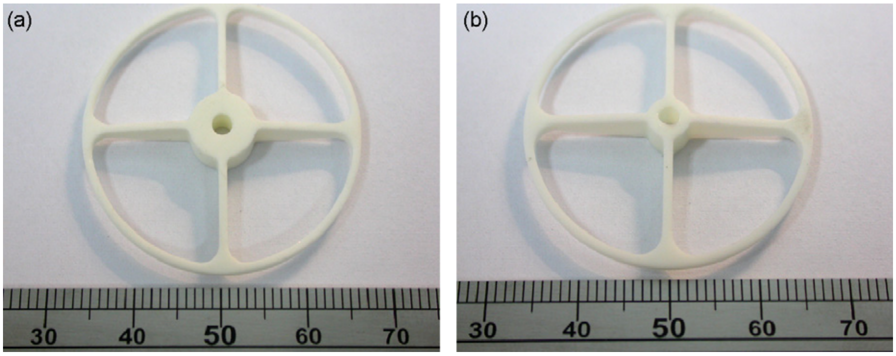

Fig. 9. Two prototypes of SDVA; (a) SDVA II, (b) SDVA III.

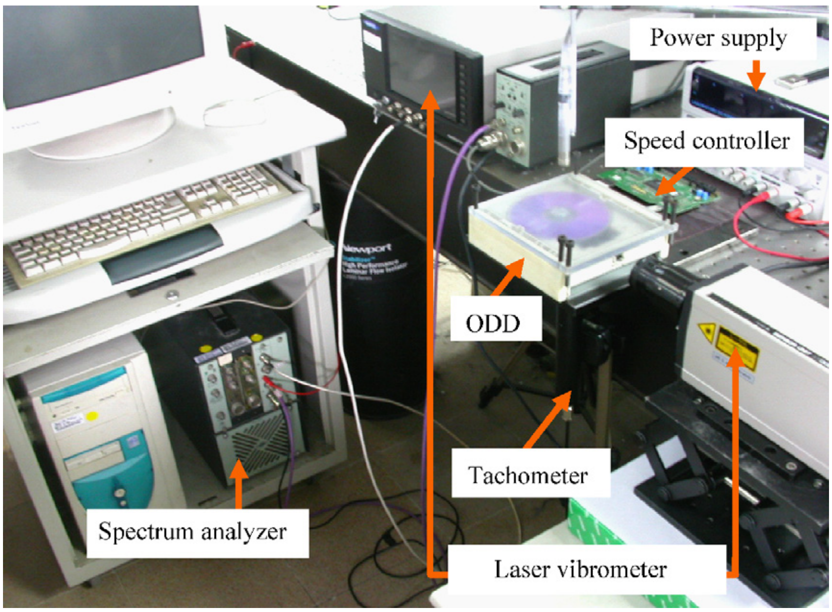

Fig. 10. Experiment setup.

5700 to 8400 rev/min, whereas the SDVA III was designed for the higher rotational speed ranged from 7500 to 10,200 rev/min, respectively. The ratios of the natural frequency of the SDVA II and SDVA III to the excitation frequency of the rotating disk are all in the range from 0.95 to 1.05. Therefore, the SDVA II and the SDVA III both can effectively suppress the vibration caused by the disk imbalance in the specific range of the rotating speed.

6. Experimental validation

Figs. 9(a and b) show two prototypes, SDVA II and SDVA III, based on the design determined as mentioned in the previous section. Both of them were made of PU by using a mold and their material properties are listed in Table 6. An experiment was setup as shown in Fig. 10 to test the effectiveness of SDVA in reducing the vibration caused by the imbalance of optical disk. The SDVA was installed on the shaft of an ODD below the disk as shown in Fig. 11. A laser vibrometer is used to measure the vibration of the motor

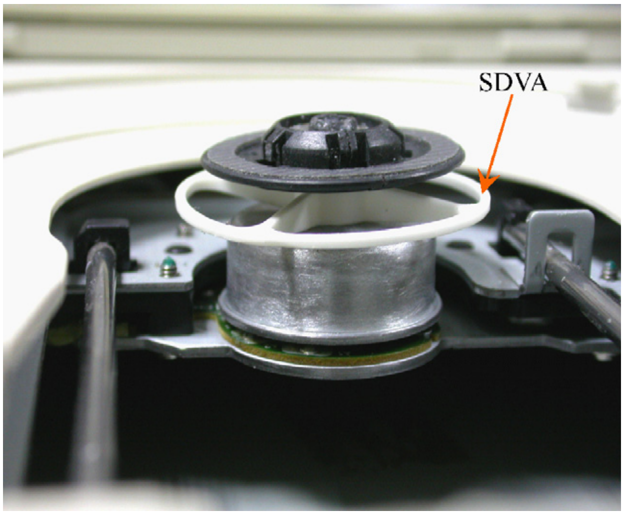

Fig. 11. An ODD with a SDVA installed.

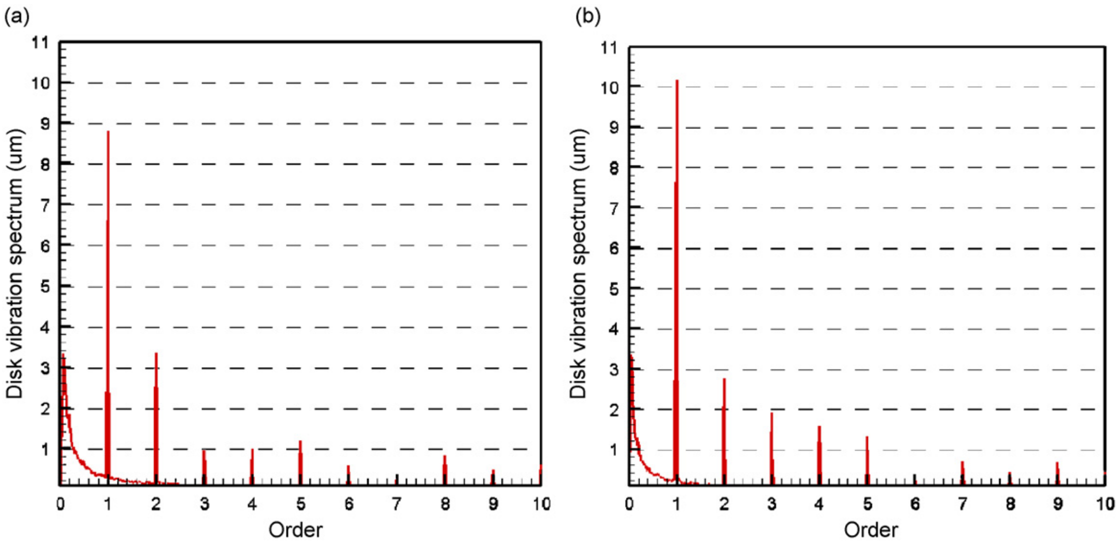

Fig. 12. Disk vibration order spectra without SDVA at (a) 6000 rev/min and (b) 10,000 rev/min.

shaft at the position very close to the rotating disk. Note that the displacement of the motor shaft in the radial direction is used to represent the disk radial vibration instead of the disk itself because the disk is too thin for the laser to focus during the rotation. A small hole was drilled beneath the ODD to allow an optical tachometer to measure the shaft rotating speed. With the information of disk rotating speed and the related vibration displacement of the rotating shaft, the shaft vibration in the radial direction is represented using order spectra to avoid smear caused by the unstable rotating speed.

The radial vibration order spectra of the rotating shaft without SDVA at 6000 and 10,000 rev/min are shown in Fig. 12. One may note that the vibration response is dominated by the first three orders; and the first order which is usually regarded as a result due to imbalance is the largest among them. The vibration order

Table 7
Disk radial vibration of first three orders

Rotational speed (rev/min)	Order	W/O absorber (μm)	With SDVA II (μm) (%)	With SDVA III (μm) (%)
6000	1	8.80	7.22 (−17.95)	8.06 (−8.41)
	2	3.33	2.50 (−24.92)	4.65 (39.64)
	3	0.95	0.89 (−6.32)	0.74 (−22.11)
7000	1	9.23	5.33 (−42.25)	6.69 (−27.52)
	2	2.88	2.63 (−8.68)	3.65 (26.74)
	3	1.85	1.55 (−16.22)	2.09 (12.97)
8000	1	10.11	4.76 (−52.92)	4.42 (−56.28)
	2	2.54	1.39 (−45.28)	2.94 (15.75)
	3	1.30	0.70 (−46.15)	1.85 (42.31)
9000	1	11.39	6.13 (−46.18)	3.44 (−69.80)
	2	2.54	2.84 (11.81)	1.54 (−39.37)
	3	1.82	1.32 (−27.47)	1.19 (−34.62)
10,000	1	10.16	6.35 (−37.50)	2.75 (−72.93)
	2	2.74	0.98 (−64.23)	2.03 (−25.91)
	3	1.90	0.18 (−90.53)	0.94 (−50.53)

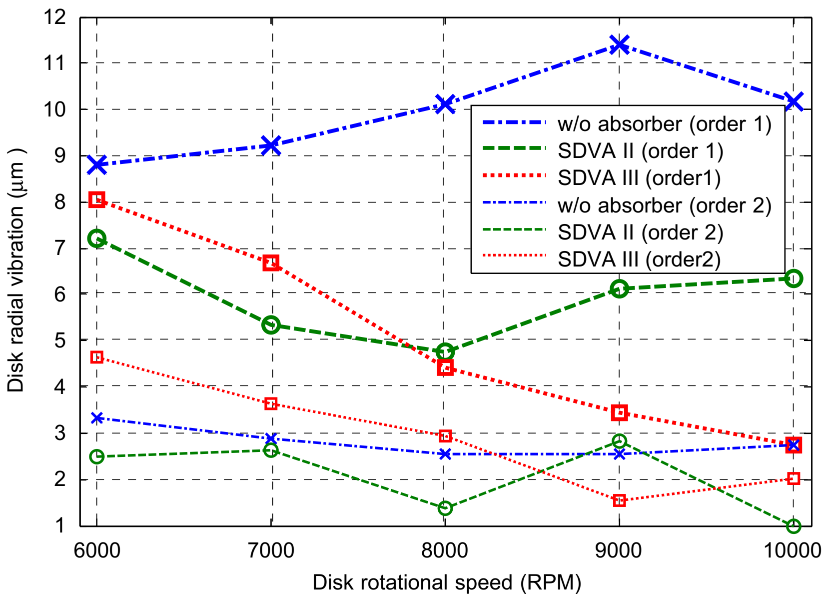

Fig. 13. Disk radial vibration of first two orders before and after SDVA being installed.

spectra of the shaft with and without SDVA were investigated for five different rotational speeds, 6000, 7000, 8000, 9000 and 10,000 rev/min, respectively. Table 7 lists the vibration amplitude of the first three orders of the shaft with and without the SDVA, and Fig. 13 illustrates their comparisons for the first two orders. It concludes that both SDVAs can effectively reduce the first-order radial vibration of the shaft at varying speeds starting from 6000 to 10,000 rev/min as expected. As a comparison, the SDVA III performs better than SDVA II at a speed above 8000 rev/min. One may also note that the vibrations corresponding to the second and the third orders of ODD with SDVA III are larger than those without a vibration absorber at certain rotational speeds. Since the vibration amplitude of the first order is much larger than those of higher orders and thus, as an overall estimate, the ODD vibration is still much reduced by using a SDVA.

7. Conclusions

A novel design of a vibration absorber used in reducing the disk vibration caused by the imbalance is proposed. It provides an alternative in countering imbalance of the disk besides the traditional ABB. The proposed vibration absorber is installed at the same position as the traditional ABB. It rotates with the disk; therefore its natural frequency varies with the rotating speed due to the change of in-plane stress caused by the centrifugal force. The objective is to make the first radial natural frequency of the absorber coincide with the rotating speed of the optical disk in a specific rotational frequency range. This design task is accomplished using shape optimization technique. Results from numerical simulations and experiments show that the proposed vibration absorber can effectively suppress the imbalance of the optical disk when the ODD operates in the specific frequency range. Moreover, as compared to the traditional ABB, it has a much simpler mechanism and can be fabricated using an injection mold machine in a cost-effective manufacturing process.

Acknowledgments

This work was partially supported by the National Science Council of Taiwan, Republic of China under Contract no. NSC 95-2221-E-061.

References

[1] M. Kiyoshi, M. Kazuhiro, Y. Shuichi, F. Michio, U. Tokuaki, K. Nasaaki, Japanese Patent 10,083,622. Disk Drive Device, 1997.
[2] K. Masaaki, Japanese Patent 10,208,374. Disk Device, 1998.
[3] Y. Takatoshi, Japanese Patent 10,188,465. Disk Drive Device, 1998.
[4] J.-R. Kang, C.-P. Chao, C.-L. Huang, C.-K. Sung, The dynamics of a ball-type balancer system equipped with a pair of free-moving balancing masses, *ASME Journal of Vibration and Acoustics* 123 (2001) 456–465.
[5] T. Majewski, Position errors occurrence in self balancers used on rigid rotors of rotating machinery, *Mechanism and Machine Theory* 23 (1) (1988) 71–78.
[6] J.-R. Kang, C.-P. Chao, C.-L. Huang, C.-K. Sung, Effects of rolling friction of the balancing balls on the automatic ball balancer for optical disk drives, *ASME Journal of Vibration and Acoustics* 127 (2005) 845–856.
[7] Y. Jinnouchi, Y. Araki, J. Inoue, Y. Ohtsuka, C. Tan, Automatic balancer (static balancing and transient response of a multi-ball balancer), *Transaction of Japan Society of Mechanical Engineers, Part C* 59 (557) (1993) 79–84.
[8] S.S. Rao, *Mechanical Vibrations*, Pearson Education, Inc., New Jersy, 2004.
[9] W.T. Thomson, M.D. Dahleh, *Theory of Vibration with Applications*, Prentice-Hall Inc., Englewood Cliffs, NJ, 1998.
[10] S.V. Hoa, Vibration of a rotating beam with tip mass, *Journal of Sound and Vibration* 67 (3) (1979) 369–381.
[11] A.A. Al-Qaisia, B.O. Al-Bedoor, Evaluation of different methods for the consideration of the effect of rotation on the stiffening of rotating beams, *Journal of Sound and Vibration* 280 (2005) 531–553.
[12] G.N. Vanderplaats, *Numerical Optimization Techniques for Engineering Design: with Application*, McGraw-Hill, New York, 1984.
[13] R.P. Brent, *Algorithms for Minimization without Derivatives*, Prentice-Hall, Englewood Cliffs, NJ, 1973, pp. 116–155.